Control Analysis and Tuning of an Industrial Temperature Control System

I. Zajic * **T. Larkowski** * **K. J. Burnham** * **D. Hill** **

* *Control Theory and Applications Centre, Coventry University, Coventry, UK (e-mail: zajici@uni.coventry.ac.uk).*
** *Abbott Diabetes Care Ltd, Witney, Oxfordshire, UK (e-mail: dean.hill@abbott.com)*

Abstract: The paper focuses on control analysis and tuning of an already installed temperature control system in a manufacturing plant. The dynamics of the investigated heating ventilation and air conditioning system are inherently nonlinear throughout the operational region. Therefore, it is challenging to tune the adopted proportional-integral controller. For this reason, a nonlinear temperature model, whose structure is predetermined based on simplified first principles assumptions, is derived. The corresponding parameters are estimated based on measured data using identification techniques. The obtained temperature model is used for off-line control analysis and subsequent control tuning.

Keywords: Air handling unit; Hammerstein model; instrumental variable; optimal tuning; proportional-integral controller; HVAC

1. INTRODUCTION

The research is concerned with heating ventilation and air conditioning (HVAC) systems dedicated for clean room production. These systems provide manufacturing areas with conditioned air such that its temperature and humidity are regulated within specified limits. Considering the complexity, nonlinear characteristics and non-stationary operational conditions of HVAC systems the control of such systems is a non-trivial task, see Underwood (1999). Most of the nonlinear HVAC systems are controlled by relatively simple proportional-integral and proportional-integral-derivative (PI/PID) controllers. In practice, the PI/PID controllers are often required to operate over a wide range of operational conditions, which commonly results in a poor control performance and can lead to increased energy consumption, see Lim et al. (2009).

Abbott Diabetes Care (ADC) UK, an industrial collaborator of the Control Theory and Applications Centre, develops and manufactures the blood glucose and ketones test strips, which are designed to assist people with diabetes, see Hill et al. (2009). One of the manufacturing requirements is that the environmental conditions during production are stable and within defined limits. To achieve this goal ADC UK utilises a number of HVAC systems for all clean room production. Preliminary investigations have revealed that the control performance of these HVAC systems, which make use of standard PI controllers, can be significantly improved by optimal tuning, see Zajic et al. (2010).

Consequently, this paper reports on a part of the research which focuses on the analysis and optimal tuning of the investigated control system with a view of subsequent implementation. The analysis is based on derived temperature models of the HVAC system and the air conditioned manufacturing area. The underlying physical relations and understanding of the investigated system at hand, play an important part in the identification of such a real-world system as well as in the control tuning. Therefore, the models are obtained based on simplified first principles assumptions with parameters estimated subsequently based on measured data. The emphasis is placed on the control analysis of the investigated system with only preliminary results presented that were obtained from the conducted optimal tuning exercise.

2. PLANT AND CONTROL DETAILS

A setup of the investigated HVAC system is shown in Figure 1. Consider Figure 1, at the point where the return air is extracted by suction from the manufacturing zone and passed through the main duct to the mixing box, in which the return air is mixed with the fresh air. The air mixture is drawn through the dehumidification unit (DU) Munster MX5000, where it is dehumidified. The dehumidified air is progressed to the AHU Wolf KG 160, where the air is heated or cooled depending on the operating requirements.

The DU comprises of a desiccant rotor, whose structure forms narrow air flutes impregnated with a moisture absorbing high performance silica gel. The dehumidification performance is adjusted by the temperature of the reactivation air, which is regulated by the gas burner. As a side effect of the DU functionality the rotor is hot and the outflow processed air is heated. The temperature of the outflow air is proportional to the reactivation air temperature. Further information on the DU functionality can be found in Zajic et al. (2010).

The AHU composes of the cooling coil, the heating coil and the main fan driven by 7.5 [kW] electric motor. During

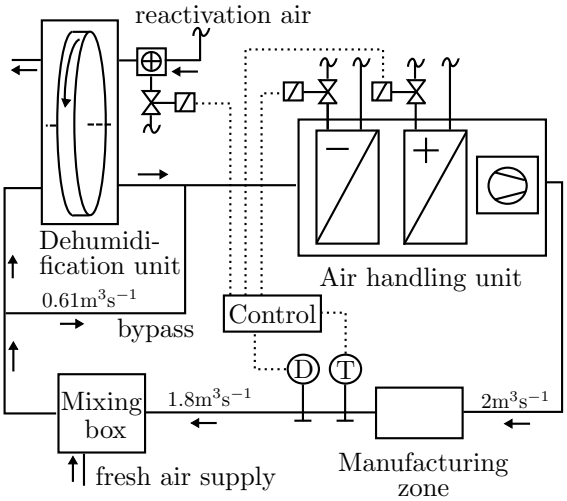

Fig. 1. Schematic diagram of the system setup.

normal operation conditions the DU provides enough heat, therefore the heating coil is disabled for most of the time. The cooling capacity of the cooling coil is regulated by means of the chilled water (having temperature of 5 [°C]) mass-flow rate being altered by the cooling valve. The heating coil works alike, however the hot water is used instead.

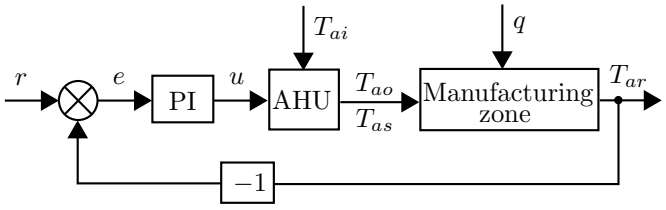

Fig. 2. Schematic diagram of the system in a control closed loop setting.

The manufacturing requirements in ADC UK are that the environmental conditions are: the air dry-bulb temperature must lie within the range 21 ± 4 [°C] and the air relative humidity must be lower than 20 [%], corresponding to a controlled dew-point temperature of -2.5 ± 3 [°C]. This paper focuses on the control analysis and optimal tuning of the temperature control loop given in Figure 2 only. There are two main components in the control loop, i.e. air handling unit (AHU) and the manufacturing zone (MZ). To simplify the system analysis only the cooling coil of the AHU is considered here as the heating coil is disabled under normal operation condition.

Considering Figure 2 the notation is as follows: inflow air temp. T_{ai}, outflow air temp. T_{ao}, supply air temp. $T_{as} = T_{ao}$, return air temp. T_{ar}, control error e, and cooling valve fractional position u in a range of $\langle 0, 1\rangle$, where 0 corresponds to a fully closed and 1 to a fully open valve. The temperature is defined in [K] or in [°C] as appropriate. The inflow air temp. is in a range $T_{ai} = \langle 20, 35\rangle$ [°C] and represents a heating load on the AHU. Heat gain acting on a manufacturing zone, denoted q [W], represents a load disturbance, which needs to be compensated by the PI controller. The designed set-point is 20 [°C] with the dead band ± 0.5 [°C]. The control set-point, denoted r, is thus $r = 20.5$ [°C] when the AHU is in a cooling mode.

3. TEMPERATURE MODEL

3.1 Air handling unit

The AHU discrete-time nonlinear model has already been derived and presented in Zajic et al. (2011). Due to space restrictions only the final identified model in a transfer function form is presented here, i.e.

$$T_{ao}(k) = \frac{b_{0,1}z^{-1}}{1 + a_1 z^{-1}} v_1(k) + \frac{b_{0,2}z^{-1}}{1 + a_1 z^{-1}} v_2(k) + o_1 + \frac{b_{0,3} + b_{1,3}z^{-1}}{1 + a_1 z^{-1}} T_{ai}(k - d_2) + \frac{b_{0,4}z^{-1}}{1 + a_1 z^{-1}} v_3(k). \quad (1)$$

Here z^{-1} denotes the backward shift operator defined such that $z^{-i}y(k) = y(k-i)$, $d_{1,2}$ denotes pure time delays expressed as an integer multiple of the sampling interval T_s, k is the discrete-time index, a_i and $b_{i,j}$ are model coefficients, and o_1 denotes a constant offset. The inputs are defined as $v_1(k) = f(u(k-d_1))$, $v_2(k) = T_{ao}(k)f(u(k-d_1))$ (bilinear-type nonlinearity), and $v_3(k) = T_{ai}(k-d_2)f(u(k-d_1))$. The function $f(\cdot)$ represents the valve static characteristic (Hammerstein-type nonlinearity) and is assumed that it can be described by a 6^{th} order polynomial

$$f(u(k)) = \sum_{p=1}^{6} \alpha_p u^p(k), \quad (2)$$

where $\alpha_{1,\ldots,6}$ are the coefficients.

The parameters of AHU model, given in (1) and (2), are estimated with a sampling time interval $T_s = 5$ [s] and are as follows: $a_1 = -0.9846$, $b_{1,0} = -0.2599$, $b_{2,0} = -0.03$, $b_{3,0} = -0.0808$, $b_{3,1} = 0.0904$, $b_{4,0} = 0.0022$, $o_1 = 10.48$ [°C], $\alpha_1 = -0.0189$, $\alpha_2 = 15.94$, $\alpha_3 = -64.06$, $\alpha_4 = 103.1$, $\alpha_5 = -71.67$, $\alpha_6 = 17.68$, $d_1 = 12$ and $d_2 = 1$ samples.

3.2 Manufacturing zone

A lumped parameter modelling approach has been adopted in which the manufacturing zone is assumed to behave as a perfectly mixed vessel. In this case the zone air temperature is homogenous in an entire zone volume and equal to the return air temperature T_{ar}. Consequently, the energy balance equations for the zone are given by

$$C_1 \frac{\mathrm{d}T_{ar}(t)}{\mathrm{d}t} = m_a c_a \left[T_{as}(t) - T_{ar}(t)\right] - U_1 A \left[T_{ar}(t) - T_w(t)\right] + q(t), \quad (3a)$$

$$C_2 \frac{\mathrm{d}T_w(t)}{\mathrm{d}t} = U_1 A \left[T_{ar}(t) - T_w(t)\right] - U_2 A \left[T_w(t) - T_a(t)\right], \quad (3b)$$

where C_1 $[J/K]$ is the thermal air capacity, C_2 $[J/K]$ thermal wall capacity, c_a $[J/kgK]$ air specific heat capacity, m_a [kg/s] air mass-flow rate, $U_{1,2}$ $[J/m^2K]$ heat transfer coefficients, t $[s]$ time, A $[m^2]$ is the effective surface of the walls, T_w [K] mean wall temp., T_a [K] ambient temperature.

The model (3) is of a second order having a fast and a slow mode. The fast mode corresponds to the air thermal capacity and the slow mode to the wall thermal capacity. Therefore, a continuous-time system identification is preferred. Defining differential operator $s^p x(t) = \mathrm{d}^p x(t)/\mathrm{d}t^p$ and eliminating for unknown wall temperature $T_w(t)$ in

(3), the model (3) can be conveniently written in a transfer function form as

$$T_{ar}(t) = \frac{b_{0,1}s + b_{1,1}}{s^2 + a_1 s + a_2}\left(T_{as}(t) + \frac{1}{m_a c_a}q(t)\right) + \frac{b_{0,2}}{s^2 + a_1 s + a_2}T_a(t). \quad (4)$$

During the data collection experiment no heat gains were acting on the system, i.e. $q(t) = 0$. Further, the ambient temperature $T_a(t)$ has not been measured, however it is expected that it can be considered as constant over the duration of the system identification experiment, i.e. $T_a(t) \simeq T_a$. Consequently, T_a effectively introduces a constant offset in measurements. The constant offset can be eliminated by subtracting the bases of measured signals in steady state prior to parameter estimation. Therefore, the final zone temperature model is given by

$$T_{ar}(t) = \frac{b_0 s + b_1}{s^2 + a_1 s + a_2}T_{as}(t - d_3) + o_2, \quad (5)$$

where d_3 denotes a pure time delay, $b_0 = b_{0,1}$, $b_1 = b_{1,1}$, and o_2 denotes an offset. Note that the sum of steady state gains (SSG) of the first and the second transfer function in (4) is equal to unity, i.e. $SSG_1 + SSG_2 = 1$. Hence, by knowing the SSG_1, the unknown offset can be calculated as

$$o_2 = \left(\overline{T}_{ar} - SSG_1\overline{T}_{as}\right), \quad (6)$$

where $\overline{T}_{as}$ and $\overline{T}_{ar}$ denotes the subtracted bases of $T_{as}(t)$ and $T_{ar}(t)$, respectively.

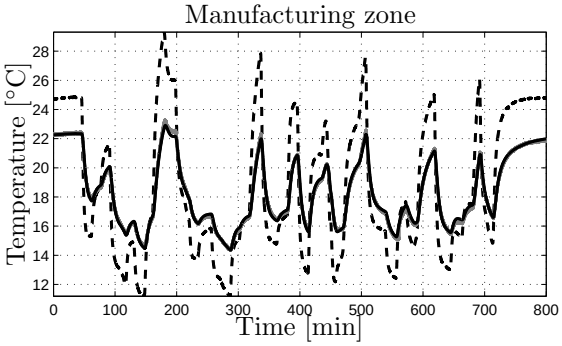

Fig. 3. Measured manufacturing zone supply air temperature (black dashed line) and zone return air temperature (grey solid line) shown together with the simulated zone return air temperature (black solid line). Estimation data set; sampling time 1 [s].

Parameter estimation The input and output signals have been acquired with a sampling time of one second, which is also the sampling time chosen for the parameter estimation. Two separate data sets have been used, one exclusively for parameter estimation and other for validation of the identified model. The measured input signals $T_{ai}(t)$ and $T_{as}(t)$ are pre-filtered using a zero-phase second order Butterworth filter with a cut-off frequency of 5^{-2} [Hz], see Gustafsson (1996), selected mainly based on a visual inspection. In order to examine the identification results two model performance criteria are used, namely, the integral of absolute error IAE [°C] defined as

$$\text{IAE} = \frac{1}{N}\sum_{k=1}^{N}|y(k) - y_s(k)| \quad (7)$$

and the coefficient of determination R_T^2 [%] given by

$$\text{R}_\text{T}^2 = 100\left(1 - \frac{\|y - y_s\|_2^2}{\|y - \overline{y}\|_2^2}\right), \quad (8)$$

where $y(k)$ denotes the measured output, $y_s(k)$ the simulated output, and N the number of samples. $\overline{y}$ is the mean value of $y(k)$, whilst y and y_s are vectors formed from $y(k)$ and $y_s(k)$, respectively.

The simplified refined instrumental variable method for continuous-time (SRIVC) system identification, see Young (2011), is used for parameter estimation of the manufacturing zone sub-model (4). The SRIVC method assumes a white additive noise disturbing the measurements and uses iteratively updated pre-filters, which effectively attenuate the noise outside the passband of the system. This method is particularly suitable for the considered application as the system input is measured and the adaptive pre-filtering helps to attenuate the influence of errors-in-variables on the estimated parameters.

To estimate the unknown pure time delay d_3 in (5) the function `rivcid` in Captain Toolbox for Matlab, Taylor et al. (2007), is utilised. This function uses the SRIVC method for the model order and delay estimation. The `rivcid` function confirms that the second order model with a single zero in the numerator is appropriate, and the estimated delay is null, i.e. $d_1 = 0$. Of course, the pure time (transport) delay is present in practice and is in order of seconds. However, in this case the delay is somewhat accommodated in the slow mode of the model and cannot be effectively estimated from the data. The obtained model parameter estimates are:

$$a_1 = 53.174 \times 10^{-4}\ (0.7327 \times 10^{-4}),$$
$$a_2 = 15.786 \times 10^{-7}\ (0.4870 \times 10^{-7}),$$
$$b_0 = 23.218 \times 10^{-4}\ (0.2586 \times 10^{-4}),$$
$$b_1 = 10.294 \times 10^{-7}\ (0.3145 \times 10^{-7}),$$

with the corresponding standard errors provided in the parentheses. The estimated model has two real poles with time constants $\tau_1 = 3.33$ [min] and $\tau_2 = 0.88$ [h] corresponding to the air thermal capacity and the wall thermal capacity, respectively. Using (6) the constant offset is determined as $o_2 = 6.17$ [°C]. Subsequently, the simulation results with $\text{R}_\text{T}^2 = 99.74$ [%] and IAE $= 0.10$ [°C] are presented in Figure 3. The performance criteria have been also evaluated for the validation data set and these are $\text{R}_\text{T}^2 = 99.65$ [%] and IAE $= 0.12$ [°C], confirming the appropriateness of the model derived.

Control tuning considerations The manufacturing zone model, given in (5), can be decomposed by partial fraction expansion into a parallel connection of two first order processes corresponding to two modes: fast mode (air thermal capacity) and slow mode (wall thermal capacity). For the purpose of the control tuning only the first process corresponding to the fast mode is of interest. Therefore, the final MZ temperature model is given by

$$T_{ar}(t) = \frac{\overline{b}_0}{s + \overline{a}_1}T_{as}(t - d_3) + o_3 T_{as}(t - d_3) + o_2, \quad (9)$$

where o_3 is the steady state contribution of the slow mode and the model coefficients are calculated as: $\overline{b}_0 = 0.00226$, $\overline{a}_0 = 0.005$, and $o_3 = 0.2$.

3.3 Heat load modelling

Considering the heat gain signal $q(t)$ in (4) and the known MZ model, given in (9), the heat load model can be expressed as

$$T_q(t) = \frac{1}{m_a c_a} \frac{\overline{b}_0}{s + \overline{a}_1} q(t), \tag{10}$$

where $T_q(t)$ denotes the heat gain temperature, i.e. the temperature rise in the MZ due to the rise of the heat gain $q(t)$. Since the MZ model is identified in a continuous-time domain the model parameters have real physical meaning. Therefore, it is possible to multiply the parameters of the identified MZ model by $1/(m_a c_a)$, hence obtaining the heat load model. From technical sheets of the AHU the designed air mass-flow rate is $m_a = 2.4082$ [kg/s] and $c_a = 1005$ $[J/kgK]$.

4. CONTROL ANALYSIS

The temperature model comprises of the AHU sub-model, given in (1) and (2), and the downstream MZ sub-model, given in (9). The heat load acting on the MZ is modelled in (10). In order to analyse the overall operation range of the investigated HVAC system the steady state system characteristic is obtained and shown in Figure 4 for $q = 0$.

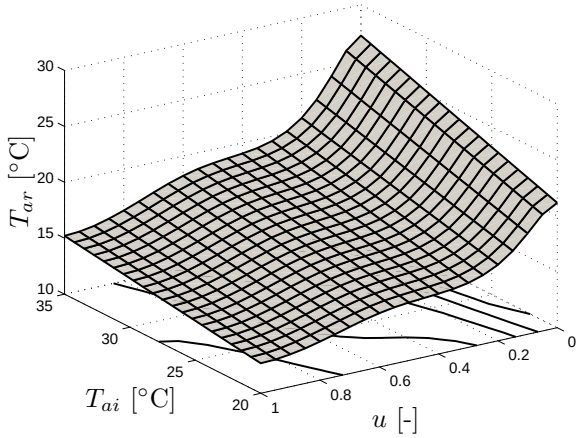

Fig. 4. The steady state characteristic of the AHU model in a series with the manufacturing zone model.

Further, it is known that the anticipated heat gain acting on the MZ is in the range of $q = \langle 0, 15 \rangle$ [kW]. Therefore, by knowing the inflow air temperature range, it is possible to calculate the operating range of the cooling valve position u. This helps to specify the HVAC system operating range for which the control system needs to be tuned more tightly. The cooling valve operating range can be determined from Figure 4 as isocline curves at a constant T_{ar}, value of which is obtained as

$$T_{ar} = r - T_q. \tag{11}$$

These steady state characteristics for the constant set-point at $r = 20.5$ [°C] are shown in Figure 5. Considering the maximal inflow air temperature $T_{ai} = 35$ [°C] and the maximal heat gain of $q = 15$ [kW], the cooling valve maximum opening is $u_{max} = 0.78$. Also by considering the minimal inflow air temperature and a zero heat gain, the minimum valve opening is $u_{min} = 0.047$.

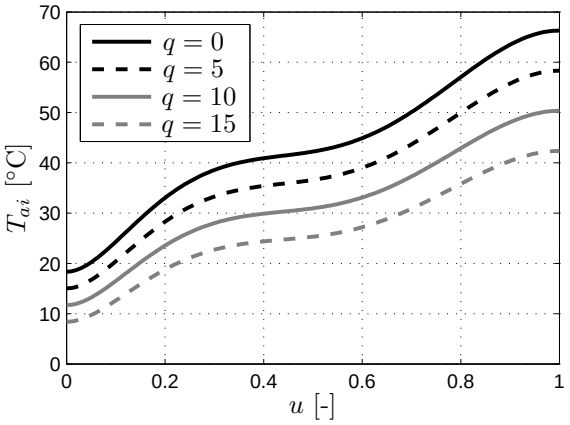

Fig. 5. System steady state characteristic for heat loads of: $q = 0$, 5, 10, and 15 kW; zone temperature set-point $r = 20.5$ [°C].

The next step in the control analysis is to obtain and plot the process steady state gain SSG [°C] and the time constant τ [s] over the operating range. These are shown in Figures 6 and 7 as black solid surfaces. The process gain and the time constant over the operating range are also obtained for the case when the cooling valve static characteristic, given in (2), is not considered. This is depicted in Figures 6 and 7 as grey solid surface.

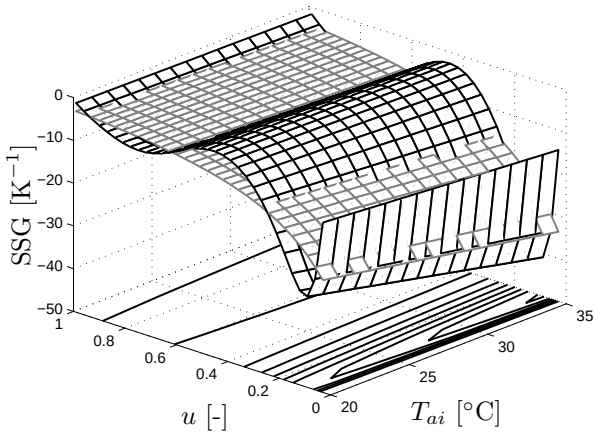

Fig. 6. Process gain of the overall system (black surface) and the corresponding process gain in the case when the static valve characteristic is ignored (grey surface).

The process gain and the time constant were obtained assuming that the nonlinear temperature model can be described sufficiently well by a first order lag plus time delay (FOLPD) linear model at a particular operating point. The linear FOLPD model is given by

$$G_p(s) = \frac{K}{s\tau + 1} e^{-sd}, \tag{12}$$

where K denotes the process gain, τ is the time constant, and d denotes the pure time delay. To simplify the analysis the delay is set to d_1, i.e. $d = d_1$. The linearised model (12) of the system has been estimated using the ordinary least squares estimation technique, see Young (2011), applied to the data recorded when the system was simulated in an

open-loop setting spanning the entire expected operating range.

The process gain SSG changes considerably in the considered operating range as observed in Figure 6. Moreover, due to the valve static characteristic the change in SSG through out the valve operating range is not monotonic and deviates as much as 1878 % looking at the smallest and the largest SSG. It can be observed in Figure 7 that the system time constant does not significantly depend on the inflow air temp. T_{ai}. Also the system time constant changes at most by 40 % in the considered operating range. Therefore, if a tight and stable control performance is required, then gain scheduled or other advanced control algorithm would be the preferred choice. The standard PI controller cannot achieve tight control performance over the assumed operating range, especially due to the large deviations in the process steady state gain.

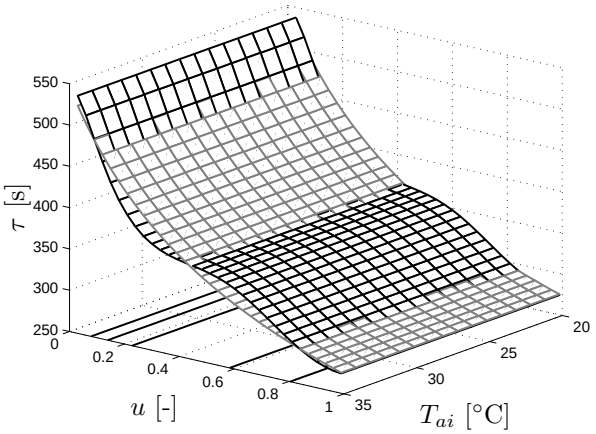

Fig. 7. Time constant of the overall system (black surface) and the time constant in the case when the static valve characteristic is ignored (grey surface).

5. OPTIMAL CONTROL TUNING

At present, the HVAC system temperature control loop uses positional form of the PI controller for a regulatory application. The structure of the ideal PI controller is

$$G_c(s) = K_c \left(1 + \frac{1}{T_i s}\right). \tag{13}$$

When implemented, the PI controller given in (13), the integral term is discretised using the Euler backward approximation, i.e.

$$\begin{aligned} e(k) &= r(k) - y(k), \\ K(k) &= K_c e(k), \\ I(k) &= I(k-1) + \frac{K_c T_s}{T_i} e(k), \\ u(k) &= K(k) + I(k), \end{aligned} \tag{14}$$

and an appropriate anti-windup logic is also adopted. The controller sampling time (rescheduling time) is set to $T_s = 5$ [s] and is the same as the sampling interval of the discrete-time temperature model. The continuous-time sub-model of the manufacturing zone is discretised using the zero-order-hold approximation method with $T_s = 5$ [s].

The system output range is $\langle 0, 4.5\rangle$ [°C], i.e. $21 + 4 - r$, and the range of the manipulated variable is $\langle 0, 100\rangle$ (from the controller perspective), where 0 corresponds to a fully closed and 100 to a fully open valve. The control requirement is to achieve tight regulation about the control set-point and a fast load disturbance rejection. Therefore, it is proposed to minimise the integral of the absolute control error IAE for the disturbance input $q(k)$, i.e.

$$\text{IAE} = \frac{1}{N} \sum_{k=1}^{N} |r(k) - T_{ar}(k)|. \tag{15}$$

In order to guarantee a minimal robustness a requirement of a minimal phase margin, denoted P_m, is imposed as a constraint during the optimisation. This represents a tradeoff between the robustness and the performance. With a higher robustness of the closed loop control system, only a larger minimal IAE can be achieved. The phase margin is selected to be relatively low, i.e. $\text{P}_\text{m} = 5°$. Otherwise, the closed loop control system tends to be too sluggish at a high-load operation condition for the current application. The optimisation was carried out at a half-load operation condition corresponding to the inflow air temperature of $T_{ai} = 27$ [°C].

The closed loop control system phase margin has been evaluated based on the selected FOLPD model. It is anticipated that the most critical FOLPD model, from the stability perspective, is that with the highest SSG. The FOLPD model at $u = 8$ [%], $T_{ai} = 27$ [°C], and $q = 0$ [W] is given by

$$G_p(s) = \frac{K}{(s\tau + 1)(sd + 1)}, \tag{16}$$

where $K = -34.8$ [K^{-1}] and $\tau = 490.1$ [s]. The Padé approximation of the time delay is used to obtain a linear transfer function, see Lim et al. (2009), hence $d = 60$ [s].

The discrete-time temperature model, given in (1), (2), and (9), is simulated in the closed loop setting together with the PI controller, given in (14), in order to find the optimal PI gains. During the simulation load disturbances of $q = 5$ [kW] and $q = 15$ [kW] are imposed. The optimisation routine computes the combination of the controller parameters which minimise the IAE performance criterion subject to constraints. The final values of the controller parameters that were obtained are

$$\begin{aligned} K_c &= -1.31 \ \ [\text{K}^{-1}], \\ T_i &= 118.08 \ \ [\text{s}]. \end{aligned}$$

These control gains indicate relatively large proportional band and a fast reset time, which is expected to be observed in the flow control application, see Kano and Ogawa (2009).

Simulation results The PI controller with the obtained optimal control gains is simulated in the closed loop setting with the temperature model under low: $T_{ai} = 20$ [°C], medium $T_{ai} = 27$ [°C], and high $T_{ai} = 35$ [°C] cooling load conditions for $r = 20.5$ [°C]. Note that the medium cooling load conditions correspond to the closed loop setting used during the control optimisation. The simulation results are given in Figures 8, 9, and 10 for low, medium, and high cooling load conditions, respectively.

As expected the controller is active under low load conditions and becomes more sluggish for higher load con-

ditions. However, it is interesting to note that under the medium load conditions in Figure 9 for load disturbance $q = 15$ [kW] the controller response is slower, than that for the high load case in Figure 10. This nonlinear effect is caused by the non-monotonic process SSG as shown in Figure 6, where the absolute value of the SSG firstly decreases and increases subsequently.

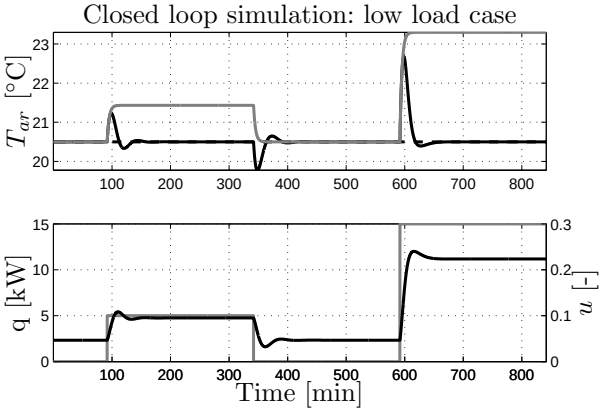

Fig. 8. The upper plot shows return air temp. T_{ar} (black solid line), set-point r (black dashed line), and heat gain temp. T_q (grey solid line) with a readjusted base at r. The lower plot shows the valve position u (black solid line) and the heat load q (grey solid line). Inflow air temperature $T_{ai} = 20$ [°C].

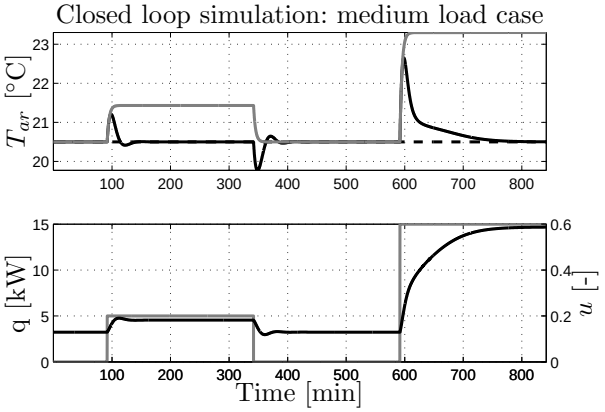

Fig. 9. The upper plot shows return air temp. T_{ar} (black solid line), set-point r (black dashed line), and heat gain temp. T_q (grey solid line) with a readjusted base at r. The lower plot shows the valve position u (black solid line) and the heat load q (grey solid line). Inflow air temperature $T_{ai} = 27$ [°C].

6. CONCLUSIONS AND FURTHER WORK

The paper has presented the control analysis and the tuning of the temperature control loop, which uses the proportional-integral controller. The control analysis revealed that the system process gain is highly nonlinear in the considered operational range and that this nonlinearity is mainly caused by the valve static characteristic. The preliminary optimal tuning exercise has shown that the use of the proportional-integral controller is possible only at the expense of a sluggish control response. As a part of the further work other control tuning techniques will

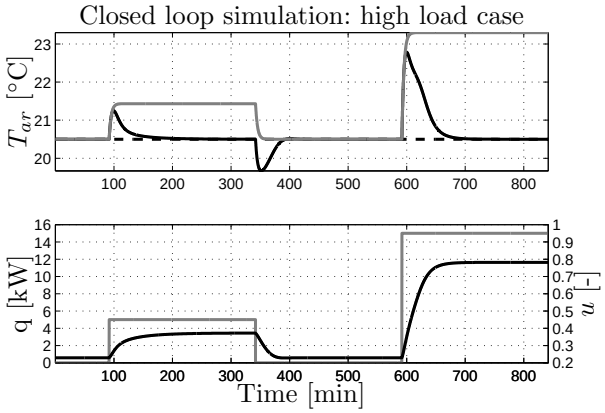

Fig. 10. The upper plot shows return air temp. T_{ar} (black solid line), set-point r (black dashed line), and heat gain temp. T_q (grey solid line) with a readjusted base at r. The lower plot shows the valve position u (black solid line) and the heat load q (grey solid line). Inflow air temperature $T_{ai} = 35$ [°C].

be investigated with the obtained controller parameters implemented on an actual plant.

REFERENCES

Gustafsson, F. (1996). Determining the initial states in forward-backward filtering. *IEEE Trans. on Signal Processing*, 44(4), 988–992.

Hill, D., Danne, T., and Burnham, K.J. (2009). Modelling and control optimisation of desiccant rotor dehumidification plant within the heating ventilation and air conditioning systems of a medical device manufacturer. In *Proc. 20th Int. Conf. Systems Engineering*, 207–212. Coventry, UK.

Kano, M. and Ogawa, M. (2009). The state of the art in advanced chemical process control in Japan. In *IFAC Symp. on Advanced Control of Chemical Processes*, 11–26. Istanbul, Turkey.

Lim, D., Rasmussen, B.P., and Swaroop, D. (2009). Selecting pid control gains for nonlinear hvac&r systems. *HVAC&R Research*, 15(6), 991–1019.

Taylor, C.J., Pedregal, D.J., Young, P.C., and Tych, W. (2007). *Environmental Time Series Analysis and Forecasting with the Captain Toolbox*. URL `www.es.lancs.ac.uk/cres/captain`.

Underwood, C.P. (1999). *HVAC control systems: Modelling, analysis and design*. E.&F.N. Spon, London.

Young, P.C. (2011). *Recursive Estimation and Time-Series Analysis: An Introduction for the Student and Practitioner*. Springer-Verlag, 2nd edition.

Zajic, I., Larkowski, T., Hill, D., and Burnham, K.J. (2010). Heating ventilation and air conditioning system: enhancement of energy consumption via control optimisation. *Systems Science*, 36(3), 40–47.

Zajic, I., Larkowski, T., Sumislawska, M., Hill, D., and Burnham, K.J. (2011). Modelling of an air handling unit: a Hammerstein-bilinear model identification approach. In *Proc. of Int. Conf. on Systems Engineering*, 59–61. Las Vegas, USA.